Science of Sintering, **48** (2016) 167-176

doi: 10.2298/SOS1602167M

UDK 666.32; 541.183

Organobentonite: Characterization and Adsorptive Properties towards Phenol and its Derivatives

Sanja Marinović [*)], Marija Ajduković, Nataša Jović-Jovičić, Predrag Banković, Zorica Mojović, Aleksandra Milutinović-Nikolić, Dušan Jovanović

University of Belgrade - Institute of Chemistry, Technology and Metallurgy, Center for Catalysis and Chemical Engineering, Njegoševa 12, Belgrade, Republic of Serbia

Abstract:

Bentonite from Mečji Do locality in Serbia was modified with hexadecyltrimethylammonium bromide (HDTMA-Br), and the sample was denoted as HDTMA-MD. The characterization of the material included X-Ray diffraction, elemental analysis and point of zero charge determination.

The adsorption of phenol and its nitro derivatives: 2-nitrophenol (2NP), 3-nitrophenol (3NP) and 4-nitrophenol (4NP) on HDTMA-MD was investigated. The adsorption capacity of HDTMA-MD toward phenol derivatives increased in the following order q_e (phenol) < q_e (3NP) < q_e (2NP) < q_e (4NP). The influence of adsorption time and initial concentration on the adsorption efficiency of HDTMA-MD was studied for 4NP. The data were best fitted with Langmuir isotherm model and the pseudo-second-order kinetic model.

Keywords: *Organobentonite, Adsorption, Phenol, Nitro phenols*

1. Introduction

Phenol and its derivatives are widely found in wastewaters from pesticides, pharmaceuticals, petroleum, petrochemical, and other industries. The quantity of phenols in wastewater is limited on 1 mg dm^{-3} by US Environmental Protection Agency [1], because phenol and its derivatives are found harmful to organisms even at low concentrations. In the last several decades the awareness of environmental pollution has increased significantly [2]. The removal of phenolic compounds from wastewater before discharge into water bodies is a necessity in order to reduce their side effects on the environment and human health. [3].

Different techniques have been used for the removal of phenol and its derivatives from aqueous solutions. Among them, adsorption is the most commonly applied because of its low initial cost, simplicity of design and ease of operation [4]. Commercial activated carbons are the most widely used in adsorption processes for the removal of phenolic compounds. Commercial activated carbons are expensive and the cost of their regeneration is high. Therefore, the bentonites could be economical alternative since they are naturally abundant low cost materials [5]. Additionally, bentonites can be modified using a variety of chemical and/or physical treatment techniques that provide materials with surface properties designed for the adsorption of specific compounds.

Interlayer cations in smectite mineral, the main constituent of bentonite, can be

[*)] **Corresponding author**: sanja@nanosys.ihtm.bg.ac.rs

exchanged with different organic cations [6, 7]. Quaternary alkylammonium cations are widely used in bentonite modification [6] providing a hydrophobic environment for the retention of organic pollutants of low polarity [8]. Numerous studies have reported the use of organobentonites as potential adsorbents for the removal of phenol from wastewater [9, 10, 11] but there is a lack of data on comparison of adsorption of different phenolic derivatives.

In this study, bentonite from Mečji Do locality in Serbia, organomodified with HDTMA-Br (denoted HDTMA-MD) was used for the investigation of the adsorption of phenol, 2-nitrophenol (2NP), 3-nitrophenol and 4-nitrophenol (4NP) from their aqueous solutions. HDTMA-Br was used for organomodification of the locally available bentonite, because when surfaces of these materials are modified by introducing long chain organic compounds, high sorption of organic contaminants can be achieved [12].

2. Experimental part

2.1. Materials

Bentonite was obtained from Mečji Do, Serbia. It was crushed, ground and sieved through a 74 μm sieve (MD). The chemical composition of the bentonite and the preparation of Na-exchanged MD (Na-MD) was reported previously [13]. The cation exchange capacity (CEC) of Na-MD, determined using the standard ammonium acetate method [14], was 0.795 mmol g^{-1}. Hexadecyl trimethylammonium (HDTMA) bromide, Alfa-Aesar, phenol, Alfa-Aesar, 2-nitrophenol (2NP), Alfa-Aesar, 3-nitrophenol (3NP), Sigma Aldrich and 4-nitrophenol (4NP), Ciba were used as received.

Organobentonite was obtained by the modification of Na-MD with HDTMA cations according to the previously reported procedure [15]. HDTMA/bentonite ratio was 1.59 mmol per 1 g of bentonite, which corresponds to 2.0 times of the value of CEC. The obtained material was denoted HDTMA-MD.

2.2. Methods

The HDTMA-MD sample was checked for its carbon, hydrogen, and nitrogen contents using a Vario EL III device (Hanau Instruments GmbH, Germany). A Philips PW 1710 X-ray powder diffractometer (Philips, The Netherlands) with a Cu anode (λ=0.154178 nm) was used for the X-ray diffraction (XRD) analysis of Na-MD and HDTMA-MD powders.

The point of zero charge (pH_{PZC}) was determined using a batch equilibration technique [16]. The dispersions of HDTMA-MD (50.0 mg of sample in 20 cm^3 of 0.01 M NaCl solution) were shaken in Erlenmeyer flasks for 24 h in a temperature-controlled water bath shaker (Memmert WNE 14 and SV 1422). The initial pH values (pH_i) were adjusted in the pH range from 2 to 11 by adding 0.1 M of HCl or NaOH solution. The pH of the solution was monitored using a "Jenway" 3320 pH meter.

2.3. Adsorption experiments

Batch-type adsorption experiments were conducted in aqueous solutions in a temperature-controlled water bath shaker. The aliquots were withdrawn at regular time intervals and the solution was centrifuged at 17000 rpm for 6 min (Hettich EBA-21). The absorbance of supernatant solutions was measured using a Thermo Electron Nicolet Evolution 500 UV-Vis. Since the UV-Vis spectra of 2NP, 3NP and 4NP vary with pH, the pH of solutions was adjusted before each UV-Vis measurement.

First, the adsorption of phenol and its three nitro derivatives (2NP, 3NP and 4NP) on

HDTMA-MD at 25 °C was investigated. The adsorption conditions were as follows: mass of adsorbent, m_{ads} = 25 mg; solution volume, v = 50.0 cm^3; adsorption time, t = 180 min; initial adsorbate concentration $C_0 = 2\times10^{-4}$ mol dm^{-3}. In the second stage, the sorption of 4NP on HDTMA-MD was monitored with respect to the initial adsorbate concentration and contact time while all other parameters were kept the same.

The amount of adsorbed substances at time t, q_t (mmol g^{-1}), was calculated from the following mass balance relationship:

$$q_t = \frac{(C_0 - C_t)v}{m_{ads}} \quad (1)$$

where C_0 and C_t (mol dm^{-3}) are the initial and the solution concentrations after sorption time t, respectively.

3. Results and Discussion

3.1. Sample characterisation

The elemental analysis revealed that the contents of C, H and N in the obtained HDTMA-MD were 15.1, 3.3 and 0.9 mass %, respectively. Also, the elemental analysis has not revealed the presence of carbon in Na-MD. Therefore, the replacement of exchangeable cations (Na^+) by quaternary ammonium cations was confirmed.

The XRD patterns of Na-MD and HDTMA-MD samples are given in Fig. 1.

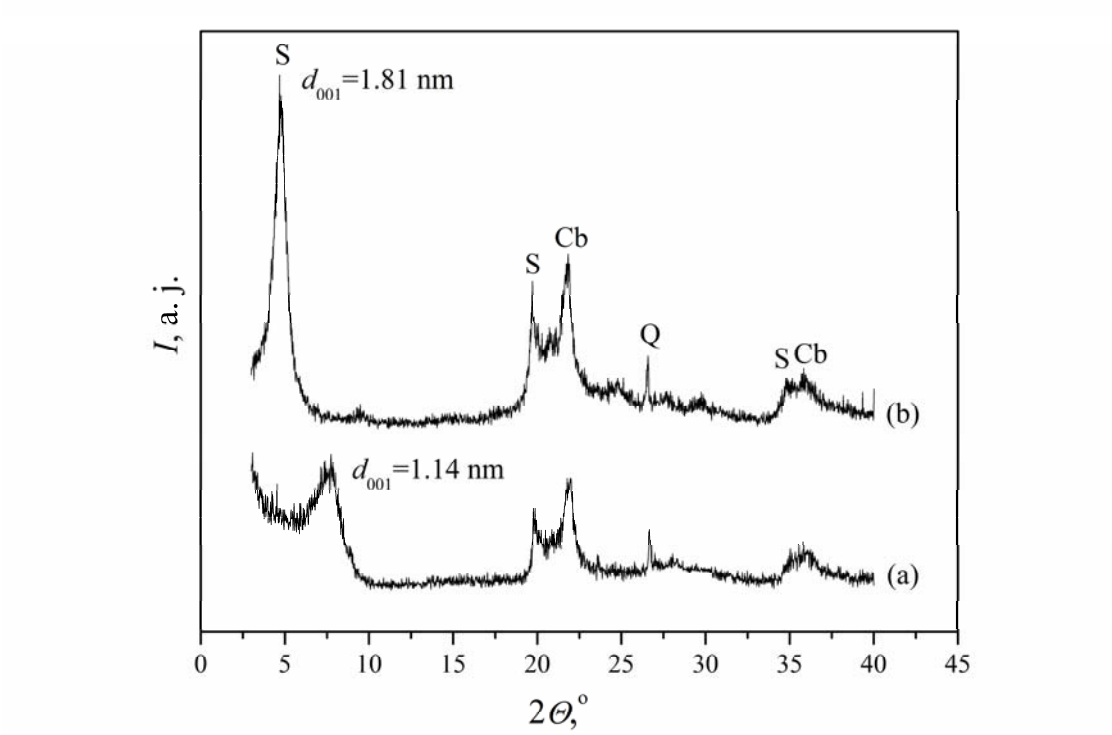

Fig. 1. XRD of Na-MD (a) and HDTMA-MD (b) samples (S: Smectite, Cb: Cristobalite, F: Feldspar, Q: Quartz).

The samples dominantly consist of smectite with minor quantities of associated minerals like cristobalite, feldspar and quartz [17]. The basal spacing (d_{001}-value) of the HDTMA-MD was larger than that of the Na-MD. This indicates that the interlamellar spacing of smectite expanded as the consequence of intercalation of HDTMA cations. The d_{001} value

of 1.81 nm for the HDTMA-MD sample corresponds to bilayer arrangement of HDTMA cations in the interlamellar space [6].

Point of zero charge for HDTMA-MD was determined to be 6.6.

3.2. Adsorption of different phenol derivatives

The data obtained for the adsorption of phenol and its nitro derivatives: 2NP, 3NP and 4NP on HDTMA-MD are given in Tab. I. It also provides pK_a and water solubility values for all investigated phenolic compounds. The amount of adsorbed substance, q_t was calculated using the equation (1).

Tab. I Adsorptive properties of phenol and its nitro derivatives.

Adsorbate	C_o mol dm^{-3}	$q_t \times 10^2$ mmol g^{-1}	%	Solubility in water g dm^{-3}	pK_a
Phenol	2×10^{-4}	1.83	4.42	80.0	9.9
2NP	2×10^{-4}	3.60	8.64	2.0	7.2
3NP	2×10^{-4}	3.43	8.57	13.5	8.4
4NP	2×10^{-4}	4.30	10.84	16.0	7.2

It can be observed that HDTMA-MD showed the highest adsorption capacity toward 4NP, and the lowest toward phenol. The lowest adsorption of phenol on HDTMA-MD is expected because of its highest solubility in water. Therefore, it could be expected that 2NP, being less soluble in water than 4NP, would be more efficiently adsorbed on HDTMA-MD. However, due to intramolecular hydrogen bonds and steric hindrance, this is not the case [18]. Considering pK_a values of all adsorbates and the fact that pH_{pzc} of HDTMA-MD is 6.6, it can be concluded that all investigated adsorbates are in molecular form, but for 2NP and 4NP the equilibrium between phenolate anion and molecular nitro phenol is more shifted to phenolate anion than for 3NP and phenol. This means that there are more phenolate anions in the 4NP and 2NP solutions. The adsorption of phenolate anions on HDTMA-MD is more pronounced than the adsorption of the corresponding molecular form. This phenomenon can be attributed to electrostatic attraction forces between HDTMA cations and phenolate anions [19].

3.3. The adsorption of 4NP

The effect of contact time on the amount of 4NP adsorbed on HDTMA-MD is presented in Fig. 2. The 4NP adsorption rate was initially high and the process then gradually slowed down. The equilibrium was reached after 20 min and $t_{1/2}$ was approx. 3 min ($t_{1/2}$ – time needed for the half of total adsorption capacity to be reached) for all investigated initial 4NP concentrations.

The 4NP adsorption rate was high at the beginning of the experiment because the adsorption sites were initially more available and 4NP could easily be adsorbed on them. After that, a slower adsorption followed as the amount of available adsorption sites gradually decreased [20].

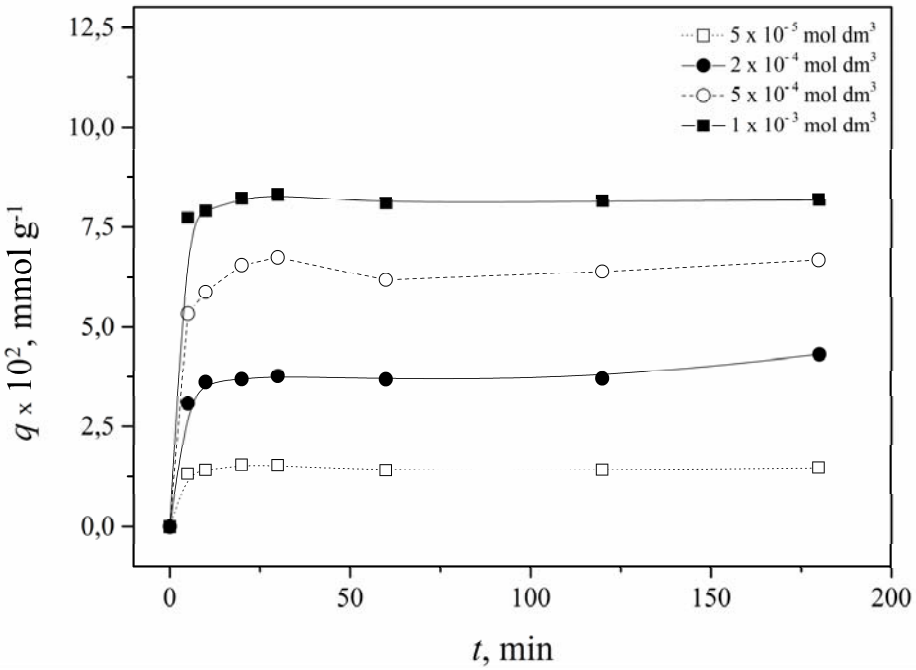

Fig. 2. The effect of contact time and different initial concentrations of 4NP on adsorption of 4NP on HDTMA-MD at 25 °C.

3.3.1. Isotherm models

Langmuir and Freundlich isotherm models were applied on the experimental data and isotherm parameters were determined. The Langmuir model [21] is a widely applied adsorption isotherm. It is represented by the following equation:

$$q_e = \frac{q_{\max} K_L C_e}{(1 + K_L C_e)} \quad (2)$$

where: q_e is the amount of adsorbed substance at equilibrium (mmol g^{-1}), K_L is the Langmuir constant related to the adsorption capacity and q_{max} is the monolayer capacity of the adsorbent.

Freundlich isotherm model [22] is an empirical model that can be applied to nonideal adsorption on heterogeneous surfaces as well as to multilayer adsorption and is expressed by the following equation:

$$q_e = K_F C_e^{\frac{1}{n_F}} \quad (3)$$

In Freundlich isotherm model K_F and n_F are isotherm parameters that characterize adsorption capacity and intensity, respectively.

Experimental data along with Langmuir and Freundlich isotherms are presented in Fig. 3.

Tab. II Calculated model constants and coefficients of determination.

Langmuir			Freundlich		
K_L dm^3 $mmol^{-1}$	q_{max} mmol g^{-1}	R^2	K_F (mmol g^{-1})/(mmol dm^{-3})$^{1/n_F}$	n_F	R^2
3.81	0.104	0.996	0.087	2.17	0.964

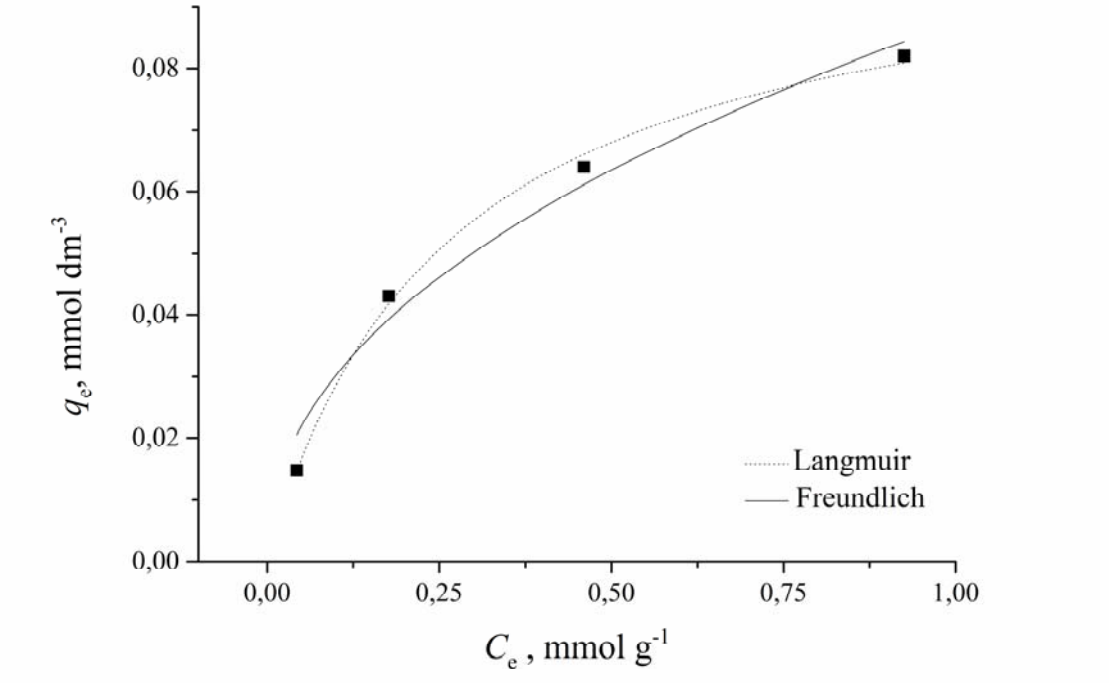

Fig. 3. Adsorption isotherms for the adsorption of 4NP on HDTMA-MD.

The isotherm parameters of each isotherm model are presented in Tab. II along with coefficients of determination (R^2).

Langmuir model better fits experimental data having R^2 close to unity and is appropriate to describe adsorption of 4NP on HDTMA-MD. The applicability of Langmuir isotherm on the experimental data indicates that the adsorption active sites on HDTMA-MD are homogeneously distributed on the surface.

3.3.2. Kinetic models

The pseudo-first-order and pseudo-second-order kinetic models were tested in the case of 4NP adsorption on HDTMA-MD. The integrated rate law for pseudo-first order and pseudo-second order reactions in linear form is presented in Eq. (4) and Eq. (5), respectively [23,24].

$$\log (q_e - q_t) = \log q_e - \frac{k_1 t}{\ln 10} \tag{4}$$

$$\frac{t}{q_t} = \frac{1}{k_2 q_e^2} + \frac{t}{q_e} \tag{5}$$

where: k_1 is the pseudo-first order rate constant (min^{-1}), k_2 is the pseudo-second order rate constant (g mmol^{-1} min^{-1}).

The parameters calculated for the pseudo-first and pseudo-second order model are presented in Tab. III.

R^2 values for pseudo-first order model are relatively low, indicating poor correlation of data with this model. On the other hand, R^2 values for the pseudo-second order model are >0.990 for all initial concentrations. Besides, q_e values, calculated from the equation for the pseudo-second order kinetic model, show good agreement with the experimental values, confirming that the adsorption of 4NP on HDTMA-MD followed the pseudo-second order kinetic model.

Tab. III Kinetic parameters for adsorption of 4NP on HDTMA-MD.

$C_i \times 10^4$ mol dm^{-3}	$q_e^{exp} \times 10^2$ mmol g^{-1}	Pseudo-first-order			Pseudo-second-order		
		k_1 min^{-1}	q_e^{calc} mmol g^{-1}	R^2	k_2 g mmol^{-1} min^{-1}	$q_e^{calc} \times 10^2$ mmol g^{-1}	R^2
0.5	1.48	7.39	1.00	0.020	3.12	1.46	0.999
2.0	4.30	4,86	1.00	0.198	0.06	4.19	0.991
5.0	6.68	4,78	0.99	0.600	0.11	6.64	0.999
10.0	8.20	5,79	0.99	0.297	1.69	8.19	0.994

3.3.3. Diffusion-based kinetic models

The most commonly used technique for identifying the mechanism involved in the adsorption process is by fitting the experimental data with intraparticle diffusion model.

According to Weber and Morris [25], the rate of intraparticle diffusion can be calculated according to the equation:

$$q_t = C_{id} + K_{id}\, t^{0.5} \quad (6)$$

where K_{id} (mmol g^{-1} min$^{-0.5}$) is the intraparticle diffusion rate constant and C_{id} represents external convective mass transfer from the bulk liquid to the surface of the solid.

C_{id} is the intercept in the equation (6) and it is proportional to the boundary layer thickness (the larger the intercept the greater the boundary layer effect).

Parameters of diffusion-based kinetic models are presented in Tab. IV.

Previous studies by various researchers [26] showed that the plot of q_t vs. $t^{0.5}$ represents multilinearity, which characterizes two or more steps involved in the adsorption process. In this study was found that there are three distinct steps. The initial region of the curve is related to the adsorption on the external surface. The second region corresponds to the gradual uptake, where the intraparticle diffusion is the rate-limiting step. The final plateau region indicates the equilibrium uptake. Applying intraparticle diffusion model in the second region, $R^2 \geq 0.966$ was obtained for all investigated concentrations.

The linear plots of q_t vs. $t^{0.5}$ did not pass through the origin. This indicates that a certain degree of boundary layer control existed. Therefore, the intraparticle diffusion process was not the only rate-limiting step and other processes controlled the rate of adsorption as well [27]. Positive values for C_{id} (Tab. IV) also indicate that boundary layer had influence on the adsorption rate [28].

Tab. IV Parameters and coefficients of determination for diffusion-based models.

4NP concentrations mol dm^{-3}	5×10^{-5}	2×10^{-4}	5×10^{-4}	1×10^{-3}
Intraparticle diffusion model				
$K_{id}\times10^2$ mmol g^{-1} min$^{-0,5}$	0.10	0.05	0.44	0.19
C_{id}, mmol g^{-1}	0.011	0.034	0.044	0.073
R^2	1.000	0.993	0.966	0.976
Boyd diffusion model				
$D_i \times 10^{14}$, m^2 s^{-1}	8.25	6.69	8.05	7.39
R^2	0.987	0.999	0.992	0.980

The contribution of boundary layer or film diffusion indicated by non-zero values of the intraparticle plot intercept is often confirmed using the model given by Boyd [29]:

$$F = 1 - \frac{6}{\pi}\sum_{n=1}^{\infty}\frac{1}{n^2}\exp(-n^2 B_t) \quad (7)$$

where F is the fractional attainment of equilibrium at time t ($F=q_t/q_e$), B_t is mathematical function of F, n is an integer that defines the infinite series solution. The approximations for B_t proposed by Reichenberg [30] are as follows:

For F values < 0.85, B_t can be calculated using the equation:

$$B_t = (\sqrt{\pi} - \sqrt{\pi - \frac{\pi^2 F}{3}}) \quad (8)$$

and for F values > 0.85:

$$B_t = -0.4997 - \ln(1 - F) \quad (9)$$

Time constant, B, values were calculated from the slope of the straight line obtained from the t vs. B_t plot [28].

$$B = \frac{D_i \pi^2}{r^2} \quad (10)$$

where D_i is the effective diffusion coefficient of 4NP in the adsorbent phase, r is the radius of the adsorbent particle, assumed to be spherical. The value of the radius (r) used for the calculation was 18.5 μm [28].

The values of the effective diffusion coefficient (D_i) were calculated using equation (10) [29] and presented in the Tab. IV along with R^2 values.

Since the plot B_t versus t did not pass through the graph origin, it can be concluded that the rate controlling step in the initial adsorption stage was film diffusion [31].

4. Conclusion

Bentonite from Mečji Do locality in Serbia was organomodified with hexadecyltrimethylammonium bromide (denoted as HDTMA-MD).

The HDTMA-MD was characterized using X-Ray diffraction and elemental analysis. The replacement of exchangeable cations (Na^+) by quaternary ammonium cations was confirmed by elemental analysis. The d_{001} value of 1.81 nm for the HDTMA-MD sample implies bilayer arrangement of HDTMA cations in the interlamellar space.

The affinity of HDTMA-MD toward phenol and its nitro derivatives increased in the following order: phenol < 3NP < 2NP < 4NP. Such behaviour could be ascribed to the solubility of these adsorbates in water, but also to their chemical structure.

The influence of adsorption time and initial concentration on the adsorption efficiency of HDTMA-MD was studied for 4NP since it showed the best adsorption on the investigated material. The adsorption was initially fast and it gradually slowed down as the equilibrium was reached. The isotherm data were best fitted using the Langmuir model, while the adsorption dynamics obeyed the pseudo-second-order kinetic model for all initial concentrations. In the first stage of the adsorption process the Boyd diffusion model could be applied on the investigated system, while in the second stage the obtained results were described well with the intraparticle diffusion model.

Acknowledgments This work was supported by the Ministry of Education, Science and Technological Development of the Republic of Serbia (Project III 45001).

5. References

1. R. I. Yousef, B. El-Eswed, A. H. Al-Muhtaseb, Chem. Eng. J., 171 (2011) 1143.

2. S. Ristić, A. Jovicević, S. Kocić, M. Spasojević, A. Maričić, Sci. Sinter., 43 (2011) 71.
3. S. Marinović, A. Milutinović-Nikolić, A. Nastasović, M. Žunić, Z. Vuković, D. Antonović, D. Jovanović, J. Serb. Chem. Soc., 79 (2014) 1249.
4. S. L. Gayatri, M. Ahmaruzzaman, Assam U. J. Sci. Technol.: Physical Sci. Technol., 5 (2010) 156.
5. S. Al-Asheh, F. Banat, L. Abu-Aitah, Sep. Purif. Technol., 33 (2003) 1.
6. G. Lagaly, M. Ogawa and I. Dékány, Clay Mineral–Organic Interactions, in: Developments in Clay Science – Volume 5A, Handbook of Clay Science (second ed.), F. Bergaya, G. Lagaly (Eds.), Elsevier Ltd., Amsterdam 2013, pp.435–505.
7. S. Stojiljković, M. Stamenković, D. Kostić, M. Miljković, B. Arsić, I. Savić, I. Savić, V. Miljković, Sci. Sinter., 45 (2013) 363.
8. Z. Li, R. S. Bowman, Environ. Sci. Techonol., 31 (1997) 2407.
9. Q. Zhou, H. P. He, J. X. Zhu, W. Shen, R. L. Frost, P. Yuan, J. Hazard. Mater., 15 (1–3) (2008) 1025.
10. M. Huang, R. Zhu, Adsorpt. Sci. Technol., 29 (2011) 29.
11. L. Zhu, B. Chen, X. Shen, Environ. Sci. Technol., 34 (3) (2000) 468.
12. V. Sreedharan, P. V. Sivapullaiah, Indian Geotech J., 42(3) (2012) 161.
13. M. Žunić, A. Milutinović-Nikolić, D.. Stanković, D. Manojlović, N. Jović-Jovičić, P. Banković, Z. Mojović, D. Jovanović, Appl. Surf. Sci., 313 (2014) 440.
14. Environmental Protection Agency, 1986. Method 9080 - Cation exchange capacity of soils (ammonium acetate). Available from http://www.epa.gov/osw/hazard/testmethods/sw846/pdfs/9080.pdf (verified 14 March 2013)
15. N. Jović-Jovičić, A. Milutinović-Nikolić, P. Banković, Z. Mojović, M. Žunić, I. Gržetić, D. Jovanović, Appl. Clay Sci., 47 (2010) 452.
16. S. K. Milonjić, A. L. Ruvarac, M. V. Šušić, Thermochim. Acta, 11 (1975) 261.
17. D. M. C. MacEwan, M. J. Wilson, Interlayer and intercalation complexes of clay minerals, in: Crystal Structures of Clay Minerals and Their X-ray Identification, G. W. Brindley, G. Brown (Eds.), Mineralogical Society, London 1980, pp. 197–248.
18. C. Moreno-Castilla, J. Rivera-Utrilla, M. V. Lopez-Ramon, F. Carrasco-Marin, Carbon 33 (1995) 845.
19. U. F. Alkaram, A. A. Mukhlis, A. H. Al-Dujaili, J. Hazard. Mater., 169 (2009) 324.
20. H. B Senturk, D. Ozdes, A. Gundogdu, C. Duran, M. Soylak, J. Hazard. Mater., 172 (2009) 353.
21. I. J. Langmuir, J. Am. Chem. Soc., 40 (1918).1361.
22. H. M. F. Freundlich, J. Phys. Chem., 57 (1906) 385.
23. S. Lagergren, „Zur theorie der sogenannten adsorption gelöster stoffe", Kungliga Svenska Vetenskapsakademiens, Handlingar 24 (1898) 1.
24. P. K. Malik, Dyes Pigm., 56 (2003) 239.
25. W. J. Weber Jr., J. C. Morris, J. Sanit. Eng. Div. Am. Soc. Civ. Eng., 89 (1963) 31.
26. O. S. Bello, S. Afr. J. Chem., 66 (2013) 32.
27. I. D. Mall, V. C. Srivastava, N. K. Agarwal, I. M. Mishra, Chemosphere 61 (2005) 492.
28. A. Milutinović-Nikolić, D. Maksin, N. Jović-Jovičić, M. Mirković, D. Stanković, Z. Mojović, P. Banković, Appl. Clay Sci., 95 (2014) 294.
29. G. E. Boyd, A. W. Adamson, L. S. Myers, J. Am. Chem. Soc., 69 (1947) 2836.
30. D. Reichenberg, J. Am. Chem. Soc., 75 (1953) 589.
31. S. Kumar, N. Rawat, A. S. Kar, B. S. Tomar, V. K. Manchanda, J. Hazard. Mater. 192 (2011) 1040.

Садржај: *Бентонит, са локалитета Мечји До у Србији, је модификован хексадецил триамонијум бромидом (HDTMA-Br) и узорак је означен као HDTMA-MD. Карактеризација материјала је обухватила дифракцију X-зрака, елементалну анализу и одређивање тачке нултог наелектрисања.*

Испитивана је адсорпција фенола и његових нитро деривата: 2-нитрофенола (2NP), 3-нитрофенола (3NP) и 4-нитрофенола (4NP) на HDTMA-MD. Адсорпциони капацитет HDTMA-MD према дериватима фенола расте следећим редоследом q_e *(фенол)* $< q_e$ *(3NP)* $< q_e$ *(2NP)* $< q_e$ *(4NP). Проучаван је утицај времена адсорпције и почетне концентрације на ефикасност адсорпције 4NP на HDTMA-MD. Добијени подаци најбоље се уклапају у Лангмиров изотермни модел, док се адсорпциона динамика покорава кинетици псеудо-другог реда.*

Кључне речи: *органобентонит, адсорпција, фенол, нитро феноли*